Assessment of linear phase array HF radar in retrieving ocean surface wind and wave parameters in Taiwan Strait

Duy-Toan Dao[1], Hwa Chien*[1], Pierre Flament[2], Meng-Yuan Chen[1]

[1] Institute of Hydrological and Oceanic Sciences, National Central University, Taiwan (R.O.C.)

[2]Department of Oceanography, the University of Hawaii at Manoa, USA

Abstract

A 27.75 MHz linear array HF radar system (LERA-MKIII) consists of 16 element Rx antennas installed at the north of Taichung harbor at Taiwan's western coast in lately November 2018. The system is low-cost, size compact, easy to install and maintain. This system aims to long-time monitoring ocean wave evolution in the middle of the Taiwan Strait. In the present study, existing algorithms are implemented to retrieve ocean surface wind and wave parameters and assess the performance of the LERA system. For HF radar data processing, the algorithms of Fourier transform and beamforming techniques were first used to provide the Doppler-Range spectrum at different azimuth directions, which is the input of wave and wind parameters calculation. Further, to estimate wave parameter and wind speed, the Barrick's (1977) and Dexter and Theodorides's (1982) formulations were adopted. Based on the experience of data processing, we found that the presence of highly variable surface current might influence the bias estimation of wave and wind parameters. In order to reduce the uncertainty of surface wave and wind measurements, an adaptive method for identifying spectra component areas is proposed. This technique was developed based on Kirincich's (2017) approach that includes the pretreatment of Doppler-rang spectrums, marker-controlled watershed segmentation, and image processing technique. For assessing the uncertainty of surface wave and wind parameters estimated from backscattered radar sea-echo, the in-situ wave data measured by an AWAC and a coastal wind gauge was used. The inter-comparisons between estimated and in-situ measurements were carried out under the condition of winter monsoon and the passage of tropical cyclones. Based on comparison results, it is found that the bias of wave and wind parameters could be reduced by using the new approach, especially under the condition of varying sea surface current, severe sea state, and highly radio interference.

Keywords: high-frequency coastal radar, wave and wind parameters, the ImageFOL method.

1. Introduction

Over approximately five decades of developing, the high-frequency (HF) radar technique becomes an essential technique for coastal monitoring and relevant applications such as marine safety and coastal hazard warning. In terms of low cost, size compact, easy to install, and maintain, hundreds of coastal HF radar systems have been installed worldwide for various purposes [1, 2]. Based on the reviewed as in [2, 3], HF radars can provide high-quality and real-time data of ocean surface wave and wind measurements under various conditions such as monsoon front and the passage of Tropical storms. Also, the derived observations from HF radar sea-echo have higher spatial and temporal resolutions than those of satellite and in-situ techniques. Those data are essential information for making plans and decisions of coastal managers and emergency responders. In addition, ocean parameters estimated from coastal HF radar sea-echo are essential data for understating coastal circulation processes such as tidal flows, ocean wave evolution, wave-current interaction, and (sub)mesoscale variability [1]. It demonstrated that HF radars could play a prominent role in monitoring the dynamics of upper ocean layers in the coastal zone as well as the Exclusive Economic Zone (EEZ) area.

In theory, the radio signal at HF bands can transmit hundreds of kilometers along the ocean's salty surface, and the backscattered HF radar signal contains the information of ocean surface current and gravity waves. Then, the Fourier transform algorithm is used to transform the backscattered HF radar signal to the Doppler-range (D-R) spectrum [4], the level 1 product of the HF radar system. The Doppler spectrum characteristic has been explained in many literature reviews, such as [5, 6, 7]. From the early 1980s, the HF radar technology has been designed in different antenna types for retrieving ocean parameters. In which, the cross-loop antenna mainly developed for retrieving ocean surface current [8, 9]; and the later feature, which is linear phased-array systems, was developed to retrieve the measurement of ocean surface waves. Following the latter concept of receiving antenna, the Wave Radar (WERA) system developed by the University of Hamburg, Germany, was developed [10]. Then, the beamforming (BF) algorithms are widely used to extract the D-R spectrum at different azimuth directions. Thus, this system provides better accuracy of the D-R spectrum in terms of signal-to-noise ratio (SNR) compared to the cross-loop type system and can give better-resolved second-order information useful for estimating surface wave parameters.

In order to estimate ocean surface information from HF radar sea-echo, numerous theories have been developed [6, 7, 11, 12]. In which, Barrick's approach [5, 6, 13] is considered as the fundamental theory for representing the interaction between radio waves and

gravity waves. Subsequently, many inversion methods were developed for estimating wave parameters [14, 15, 16, 17], wave spectrum [18, 19, 20, 21], and wind speed [22, 23, 24]. In which, the Barrick's formulation [16] was developed based on the relationship between root-mean-square wave height, h_{rms}, and the ratio of the weighted 2nd-order energy over the 1st-order energy. Thus, this method was demonstrated a better for estimating wave parameters than two other empirical methods [25].

In another respect, an efficient range of wave height retrieved by HF radar techniques was suggested based on the utility of perturbation theory [16]. Following that, there exists the relationship between sea surface roughness and HF radar frequency, and the highest value of significant wave height, Hs, estimated from HF radar backscattered signal is suggested as, $H_{sat} = 2/k_0$ [13, 26, 27]. Herein, H_{sat} and k_0 are saturated significant wave height and radio wavenumber, respectively. When the practical value of significant wave height is over the saturated amount, the operating radar frequency should be switched to lower frequency bands [13, 26, 27].

As the advance of no time-consuming, no included empirical constants and robust in performance, Barrick's empirical formulas [28] are adopted for estimating wave height and period in this study. However, the uncertainty of wave parameters is not only dependent on the performance of the inversion method; it also depends on the identification of Doppler spectra components and radar spectra noise. Therefore, the detection of Doppler spectra components plays a crucial role in the accuracy of wave parameter estimation. Initially, the lower and higher bounds of given wave frequencies were suggested to separate the 1st- and 2nd-order components, and the 2nd-order component with noise [20, 29, 30, 31]. However, it may not correct under the condition of varying surface current and high background noise. Therefore, an alternative method for identifying Doppler spectra components regions is adopted in this study to improve the uncertainty of wave parameters. This approach is developed based on the ImageFOL method [32] that consists of the pretreatment of the D-R spectrum, marker-controlled watershed segmentation (MCWK), and an image processing technique. This method is implemented to detect and separate the region of the 1st- and 2nd-order components from the D-R spectrum. Later, the outputs are used for retrieving wave parameters using Barrick's empirical formulas. Further, wind speed is calculated from estimated wave height and period. The estimation result of ocean surface wave and wind parameters is compared with the in-situ data to show the performance of the method as well as the HF radar system. This paper is organized as follows. Section 2 describes the dataset and methodology; the results and discussions are represented in Section 3. Finally, Section 4 is the conclusions.

2. Datasets and Methodology

The introduction of HTCN station

In order to monitor the dynamic of upper ocean layers in the middle of Taiwan Strait for the long-term, a 27.75 MHz HF radar LERA MK III system was installed at the end of November 2018. This system is namely HTCN and located at 24° 18.591'N and 120° 31.389'E at northern of Taichung harbor (Figure 1). The transmitter is a 2×2 antenna array arranged in a rectangle shape with edges of λ/2 and λ/4, with λ is radio wavelength. The transmitter signal is Frequency-modulated continuous wave (FMCW) chirps. For the receiver antenna, a linear phased array consists of 16-active antennas was arranged with 4 meters of distance spacing. Other information on the HTCN station was represented in [33]. Based on the antenna type of the HTCN station, the beamforming algorithm is adopted to extract the D-R spectrum in different azimuth directions. Thus, it is the level 1 product of HF radar systems and presents the radar echo intensity distribution in terms of the radar cross-section over the dimensional of range and Doppler frequency. For obtaining the information of surface current, wave parameters, the D-R spectrum is first extracted from time-series (I & Q) data of backscattered HF radar signal (Figure 2). The step of retrieving the D-R spectrum at Rx antennas was represented and explained in [33]. Later, the conventional beamforming algorithm is implemented to get the D-R spectra at different azimuth directions.

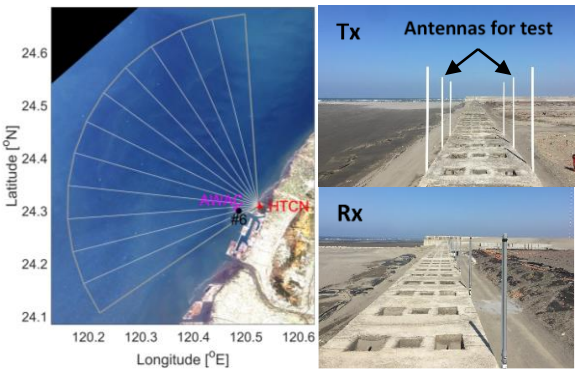

Figure 1. This figure shows the location and concept of HTCN station. Herein, the red triangle at the left panel represents HTCN's location; the gray line shows the coverage area of HTCN station; the black dot and number represent the site and name of the wind anemometer, respectively; the magenta triangle notes the position of an AWAC. The concept of Tx & Rx was represented at the upper and lower right panels, respectively.

In-situ wave and wind data

A wind anemometer measures the wind data on the top of the Taichung harbor lighthouse (24° 17.980'N, 120° 29.188'E) (Figure 1). Besides, the wave data is recorded by an Acoustic Wave And Current profiler (AWAC) (24° 18.199'N, 120° 28.916'E, -30 m depth), which is stayed in the footprint of HTCN station. The AWAC was deployed and currently working near the mouth of the Taichung harbor for long-term monitoring of the current and wave situation outside the harbor.

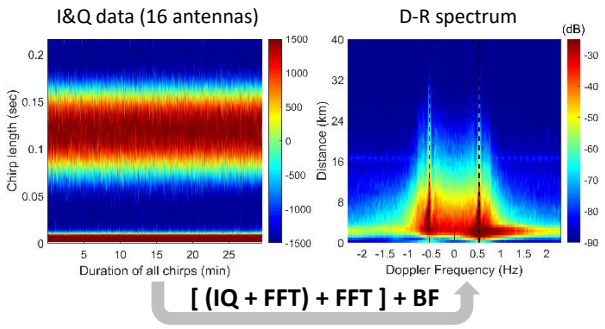

Figure 2. The flowchart shows the HF radar signal-processing concept for extracting the D-R spectrum at different azimuth directions. IQ represents the I & Q data of HF radar backscattered signal, FFT and BF represent the Fast Fourier Transform and beamforming algorithms, respectively.

The method of wave parameters estimation

In order to estimate the parameter of the ocean surface wave from HF radar sea echo, Barrick's empirical approach [16] is implemented in this study. Firstly, the root-mean-square wave height, H_{rms}, is estimated Dopper spectral, and given as follows:

$$H_{rms} = \frac{1}{k_0}\left(\frac{2\int_{-\infty}^{\infty}\sigma^{(2)}(\omega)/w(\eta)d\omega}{\int_{-\infty}^{\infty}\sigma^{(1)}(\omega)d\omega}\right)^{1/2} \quad (1)$$

In which, $\sigma^{(1)}$ and $\sigma^{(2)}$ are the first- and second-order components in the Doppler spectra, ω is the Doppler frequency, $w(\eta)$ is called the weighting function, η is the normalized Doppler frequency by dividing to Bragg frequency. The weighting function is calculated following [16], or re-digitized as in [34]. Then, significant wave height is simply determined based on the theory of ocean surface waves.

Secondly, the formulation of mean period estimation was given as:

$$T_m = \frac{2\pi}{\omega_B}\left(\frac{\int_{0,1}^{1,\infty}\sigma^{(2)}(\omega)/w(\eta)d\eta}{\int_{0,1}^{1,\infty}|\eta-1|\sigma^{(2)}(\omega)/w(\eta)d\eta}\right) \quad (2)$$

Where, the limit range of the integral in equation (2) could be either 0 to 1 or 1 to infinity.

The method of wind speed estimation

In order to estimate wind speed from the backscattered data of the HF radar system, we are going to apply Dexter & Theodorides's approach [22] in this study. In this method, the wind speed is estimated from estimated wave height and mean period based on the derivation in [22], and given as:

$$U_{10} = 9.11\times10^3\left(\frac{H_S^2}{gT_p^3}\right) \quad (3)$$

Where g is the gravity acceleration, Hs is estimated from Doppler spectra using equation (1), Tp is the peak period that can be determined from the mean period estimated by using equation (2). Based on the work of Dexter and Theodoridis [22], the relationship between peak frequency, f_p, and mean frequency, f_{m01}, under the JONSWAP's condition [35] is given as:

$$f_{m01} \simeq 1.25 f_p \quad (4)$$

Here, equation (4) was chosen as a mean between fully developed and fetch-limited cases [22].

The method of spectral component idetification

As we mentioned above, the uncertainty of wave parameters estimated from Doppler spectra also depends on identifying spectral components. The first-order peaks can easily be determined by using the method in [10]. For separating spectra components, the region of 1st-order features is initially identified based on the lower bound of given inversion wave frequency [13, 26, 27]. Thus, the approach is often sufficient for identifying the 1st-order area in case of lower HF frequency bands, simple and weak surface current, low sea-state, and high signal-noise ratio (SNR). But, it might be insufficient for higher operating radar frequency band, with higher variable surface current and severe sea-state, or strongly background noise [32]. Besides, other spectral noise influenced by intermittent radio frequency, ionospheric effect, ship echo, and offshore wind energy structures can affect the existing approach's performance.

In order to improve the identification of the 1st-order regions, an alternative method was proposed to separate the areas of spectral energy, which relevant to surface current radial velocity, from spectral energies relate to the wave field, and is called the ImageFOL method [32]. The procedure consists of a single and globally relevant smoothing length scale for reducing the amount of user-defined parameters, careful pretreatment of D-R spectra, maker-controlled watershed segmentation, and a technique of image processing. For the processing level 1 product of HTCN station, the necessary parameter of this technique is shown in Table 1.

Table 1. The setup parameters for the ImageFOL method

Name	HTCN
Transmitter frequency (MHz)	27.75
Bandwidth (KHz)	300
Doppler frequency bins	2048
Bearing angle (degree)	296 ± 60
Range resolution (km)	0.5
Angular resolution (degree)	5
v_incr (cm/s)	1.22
Complicating issues	highly complicated surface current, varying wave field, strong background noise
max_vel (cm/s)	120
vel_scale (cm/s)	20
The min SNR of 1st-order components (dB)	5

After implementing the ImageFOL method, an example of isolating first-order regions on the D-R spectrum map was shown as in Figure 3. We found that the ImageFOL method was only implemented to identify 1st- order regions, which help determine the value and azimuth direction of ocean surface current using MUSIC

algorithms [32], but it can also capture the area of higher-order components. This issue strongly affects the estimation results of wave parameters. Therefore, we have added a simple solution, which was developed based on the concept of higher spectra detection technique and correctly identified the centroid of Bragg frequencies, for assessing re-identification of 1st- order regions from estimated regions in the previous step. The example of the corrected result was shown in Figure 3.

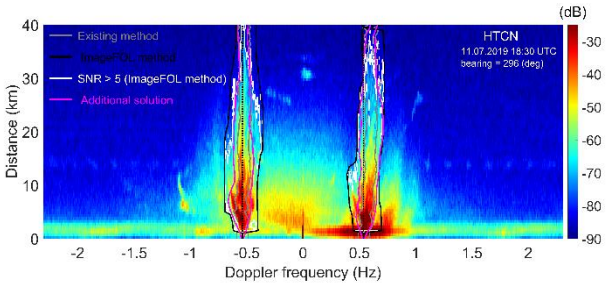

Figure 3. This figure shows the example of identifying 1st-order regions on the D-R spectrum using the ImageFOL method under the condition of highly variable surface current and normal sea-state (Hs = 0.78 m). The grey lines represent the results of the existing method; the black lines are the output of Kirincich's approach; the white lines show the region having SNR higher than 5 dB. The magenta lines show 1st-order regions by using an additional technique. The dotted black lines represent the ideal value of Bragg frequencies.

However, this method was only implemented for identifying areas of 1st-order peaks, which help to estimate the value and azimuth direction of ocean surface current; but it can also capture the part of higher-order components. This issue strongly affects the estimation results of wave parameters. Therefore, we have added a simple solution, which was developed based on the concept of higher spectra detection technique and correctly identified the centroid of Bragg frequencies, for assessing re-identification of 1st-order regions from estimated regions in the previous step (magenta lines in Figure 3).

After finishing the spectra component identification step, the output is used to estimated wave parameters by using equation (1), (2). In which, the wave frequency is given in the range of 0.07~0.45 Hz. Finally, the output wind speed is calculated from estimated Hs and Tm using equation (3). The output results are compared with in-situ measurements to assess the uncertainty of estimated wind and wave parameters and the LERA radar's performance. The comparison results will be represented in the next section.

3. Results and Discussion

In order to assess the quality of wind and wave parameters estimation, the result of estimated Hs, Tm, and wind speed were compared with those of in-situ measurement in time series data. Two selected periods of time-series data are from March 23 to April 24, 2019, at the late winter seasons (Figure 4); and July 14 to August 23, 2019, at summer seasons (Figure 5). In the first period, many winter monsoons even happened, but not strong compared with the time in January. For the second period, there exists a complex surface current near the Taichung harbor. Besides, The sea-state in this area was also influenced by Tropical depression DANAS and supper typhoon LEKIMA.

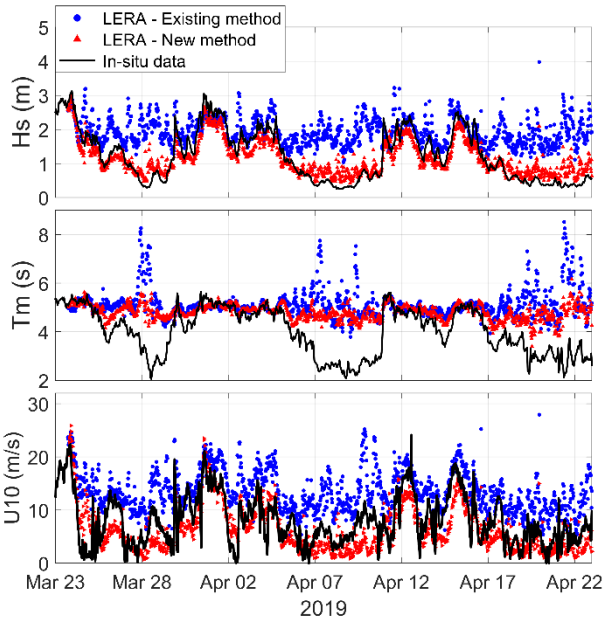

Figure 4. The time series of estimated significant wave height, period, and wind speed from the HTCN station and those of in-situ measurements under several winter monsoon events.

The comparison results of significant wave height estimation were represented in Table 2. The results in Figure 4 and Table 2 indicated that the uncertainty of wave and wind parameter had been improved using the proposed method of spectra components identification. In Figure 4, the estimated Hs (red triangle) is good agreement with the in-situ Hs (black line). Still, the estimated mean period is overestimation when the real mean wave period is lower than 4 seconds. Consequently, estimated wind speed is fit with in-situ measurement during monsoon events, and underestimate in the condition of low sea-state. In addition, there are some obvious outliers in the time series data of estimated Hs (on July 19, 2019). It may be due to the substantial interference caused by radio communication from humans near the radar station or the significant background noise.

On the other hand, Figure 5 presents the time series data of estimated wave and wind parameters compared with those of in-situ data during summertime. It is easy to see that there is much uncertainty of estimated Hs and Tm using the existing spectra component identification method, especially in normal and low sea-state. The complex of ocean surface current may play the role key for the expansion and decline in energy of the first-order peaks. And the offset method [29, 30] cannot cover the region of 1st-order peaks (Figure 3). Also, a part of the first-order area was mixed with higher-order components and led to increasing the numerator value in equation (1). The expansion of 1st-order peaks not only affects the

Table 2. The statistic value of wave and wind paramters inter-comparison

Event	Ocean parameters	Method	Statistic parameters					
			r	RMSE	BIAS	SI	a	b
Winter monsoon	Hs (m)	*Existing*	0.38	0.99	-0.27	0.343	0.530	1.29
		Proposed	0.93	0.33	0.06	0.260	0.669	0.35
	Tm (s)	*Existing*	0.16	1.64	-1.14	0.230	0.586	2.7
		Proposed	0.58	1.17	-0.84	0.170	0.319	3.5
	U10 (m/s)	*Existing*	0.68	6.68	-5.77	0.240	0.832	7.1
		Proposed	0.74	3.45	1.39	0.413	0.953	-1.0
Summer season & Typhoon influence	Hs (m)	*Existing*	0.02	1.53	-1.34	0.322	0.815	1.50
		Proposed	0.78	0.45	-0.27	0.281	0.833	0.42
	Tm (s)	*Existing*	0.20	2.5	-2.13	0.216	0.928	2.4
		Proposed	0.323	1.62	-1.40	0.160	0.496	3.3
	U10 (m/s)	*Existing*	0.58	8.38	-7.29	0.281	0.990	7.4
		Proposed	0.747	3.32	0.93	0.439	1.001	-0.9

accuracy of surface current radial velocity but also reduces the power of first-order peaks, which is an essential part of the equation (1). Consequently, the estimated Hs always overestimate in summertime under the low sea-state condition. Also, the low accuracy of detecting the 1st-order area influences the mean period's estimation result, which was demonstrated by the extremely overestimate of Tm compared to the in-situ period. However, the accuracy of Hs and Tm estimated from HF radar sea-echo data was improved by using the proposed approach of spectra component identification. Of course, the uncertainty of the estimated mean period is still high. But, for low Tm value under low sea-state conditions, the HF radar system's performance is limited. Finally, the well-fitting between estimated and in-situ wind speed that was shown in Figure 5 and Table 2 demonstrated the efficiency of the new approach.

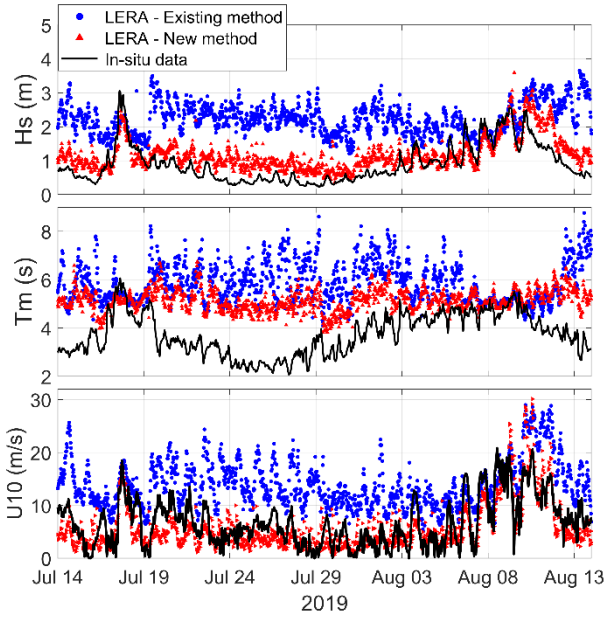

Figure 5. This figure presents the time series data of wave and wind parameters estimated from the HTCN station and those of in-situ measurements during summertime and under Tropical depression DANAS (July 18, 2020) and supper typhoon LEKIMA (August 09, 2020).

During the impact of Tropical storms, the sea-state became severe, consisting of more considerable wave height and more extended periods. The situation of surface current was controlled by typhoon waves and swell. It leads to the concentrated energy of the 1st-order peaks and well separation of spectral components. Then, the good agreement of estimated and in-situ wave parameters has demonstrated the accuracy of the estimator and the LERA system's performance. Besides, the outlier has still existed in the time-series data. It should be removed in the calculation by using some rules of the data quality control.

4. Conclusion

In this study, an alternative method used to detect the region of spectra components on the D-R spectrum was introduced and tested. Later, wave and wind estimators are implemented using Barrick's and Dexter & Theodorides's empirical formulations. The estimated wind and wave parameters were compared to those of in-situ measurement. The comparison results (Table 2) showed that the uncertainty of significant wave height, period, and wind speed was improved by using the new approach of spectral component identification. It also demonstrated this technique's potential to reduce the bias of wave parameters under the condition of complex surface current, severe sea state, and noisy radio background. Finally, the data quality control should be applied to remove the outlier caused by substantial radio interference.

5. Acknowledgment

Authors gratefully thank the Institute of Harbor and Marine Technology (IHMT), Taiwan, for providing LERA's data at the HTCN station, and the in-situ wind and wave data outside Taichung harbor.

6. Reference

[1] Rubio, A., Mader, J., Corgnati, L., Mantovani, C., Griffa, A.,

Novellino, A., *et al.*, "HF Radar Activity in European Coastal Seas: Next Steps toward a Pan-European HF Radar Network," *Frontiers in Marine Science*, Vol. 4, pp. 1-20, 2017.
[2] Roarty, H., Cook, T., Hazard, L., George, D., Harlan, J., Cosoli, S., *et al.*, "The Global High Frequency Radar Network," *Frontiers in Marine Science*, Vol. 6, 2019.
[3] Fujii, S., Heron, M.L., Kim, K., Lai, J.W., Lee, S.H., Wu, X., *et al.*, "An overview of developments and applications of oceanographic radar networks in Asia and Oceania countries," *Ocean Science Journal*, Vol. 48, pp. 69-97, 2013.
[4] Crombie, D.D., "Doppler Spectrum of Sea Echo at 13.56 Mc./s," *Nature*, Vol. 175, pp. 681, 1955.
[5] Barrick, D.E., "First-order theory and analysis of MF/HF/VHF scatter from the sea," *IEEE Transactions on Antennas and Propagation*, Vol. 20, pp. 2-10, 1971.
[6] Barrick, D.E., "Remote sensing of sea state by radar," *In: Ocean 72 - IEEE International Conference on Engineering in the Ocean Environment*, pp. 186-192, 1972.
[7] Hasselmann, K., "Determination of Ocean Wave Spectra from Doppler Radio Return from the Sea Surface," *Nature Physical Science*, Vol. 229, pp. 16, 1971.
[8] Barrick, D.E., Jerzy, L., Randy, D.C., "Mapping Surface Currents with CODAR," *Sea Technol*, Vol. 26, pp. 43-46, 48, 1985.
[9] Barrick, D.E., Evans, M., Weber, B., "Ocean surface currents mapped by radar," *In: Proceedings of the 1978 IEEE First Working Conference on Current Measurement*, pp. 59-65, 1978.
[10] Gurgel, K.W., Antonischki, G., Essen, H.H., Schlick, T., "Wellen Radar (WERA): a new ground-wave HF radar for ocean remote sensing," *Coastal Engineering*, Vol. 37, pp. 219-234, 1999.
[11] Gill, E.W. and Walsh, E.J., "High-frequency bistatic cross sections of the ocean surface," *Radio Science*, Vol. 36, pp. 1459-1475, 2001.
[12] Voronovich, A.G. and Zavorotny, V.U., "Measurement of Ocean Wave Directional Spectra Using Airborne HF/VHF Synthetic Aperture Radar: A Theoretical Evaluation," *IEEE Transactions on Geoscience and Remote Sensing*, Vol. 55, pp. 3169-3176, 2017.
[13] Lipa, B. and Barrick, D.E., "Extraction of sea state from HF radar sea echo: Mathematical theory and modeling," *Radio Science*, Vol. 21, pp. 81-100, 1986.
[14] Wyatt, L.R., "Significant waveheight measurement with h.f. radar," *International Journal of Remote Sensing*, Vol. 9, pp. 1087-1095, 1988.
[15] Maresca, J.W. and Georges, T.M., "Measuring rms wave height and the scalar ocean wave spectrum with HF skywave radar," *JGR Oceans*, Vol. 85, pp. 2759-2772, 1980.
[16] Barrick, D.E., "Extraction of wave parameters from measured HF radar sea-echo Doppler spectra," *Radio Science*, Vol. 12, pp. 415-424, 1977.
[17] Graber, H.C. and Heron, M.L., "Wave height measurements from HF radar," *Oceanography*, Vol. 10, pp. 90-92, 1997.
[18] Hisaki, Y., "Nonlinear inversion of the integral equation to estimate ocean wave spectra from HF radar," *Radio Science*, Vol. 31, pp. 25-39, 1996.
[19] Hashimoto, N. and Tokuda, M., "A Bayesian Approach for Estimation of Directional Wave Spectra with HF Radar," *Coastal Engineering Journal*, Vol. 41, pp. 137-149, 1999.
[20] Howell, R. and Walsh, E.J., "Measurement of ocean wave spectra using narrow-beam HE radar," *IEEE Journal of Oceanic Engineering*, Vol. 18, pp. 296-305, 1993.
[21] Wyatt, L.R, "A relaxation method for integral inversion applied to HF radar measurement of the ocean wave directional spectrum," *International Journal of Remote Sensing*, Vol. 11, pp. 1481-1494, 1990.
[22] Dexter, P.E. and Theodoridis, S., "Surface wind speed extraction from HF sky wave radar Doppler spectra," *Radio Science*, Vol. 17, pp. 643-652, 1982.
[23] Maresca, J. and Barnum, J., "Estimating wind speed from HF skywave radar sea backscatter," *IEEE Transactions on Antennas and Propagation*, Vol. 30, pp. 846-852, 1982.
[24] Haus, B.K., Shay, L.K., Work, P.A., Voulgaris, G., Ramos, R.J., Martinez-Pedraja, J., "Wind Speed Dependence of Single-Site Wave-Height Retrievals from High-Frequency Radars," *Journal of Atmospheric and Oceanic Technology*, Vol. 27, pp. 1381-1394, 2010.
[25] Heron, S. and Heron, M. L., "A Comparison of Algorithms for Extracting Significant Wave Height from HF Radar Ocean Backscatter Spectra," *Journal of Atmospheric and Oceanic Technology*, Vol. 15, pp. 1157–1163, 1998.
[26] Wyatt, L., "High order nonlinearities in HF radar backscatter from the ocean surface," *IEE Proceedings - Radar, Sonar and Navigation*, Vol. 142, pp. 293-300, 1995.
[27] Lipa, B. and Nyden, B., "Directional wave information from the SeaSonde," *IEEE Journal of Oceanic Engineering*, Vol. 30, pp. 221-231, 2005.
[28] Lipa, B., "Derivation of directional ocean-wave spectra by integral inversion of second-order radar echoes," *Radio Science*, Vol. 12, pp. 425-434, 1977.
[29] Wyatt, L.R., Thompson, S.P., Burton, R.R., "Evaluation of high frequency radar wave measurement," *Coastal Engineering*, Vol. 37, pp. 259-282, 1999.
[30] Wyatt, L.R, Green, J.J., Middleditch, A., "HF radar data quality requirements for wave measurement," *Coastal Engineering*, Vol. 58, pp. 327-336, 2011.
[31] Gurgel, K.W., Essen, H.H., Schlick, T., "An Empirical Method to Derive Ocean Waves From Second-Order Bragg Scattering: Prospects and Limitations," *IEEE Journal of Oceanic Engineering*, Vol. 31, pp. 804-811, 2006.
[32] Kirincich, A.R., "Improved Detection of the First-Order Region for Direction-Finding HF Radars Using Image Processing Techniques," *Journal of Atmospheric and Oceanic Technology*, Vol. 34, pp. 1679-1691, 2017.
[33] Dao, D.T., Chien, H., Lai, J.W., Huang, Y.H., Flament, P., "Evaluation of HF radar in mapping surface wave field in Taiwan Strait under winter monsoon," *In: OCEANS 2019 - Marseille*, pp. 1-7, 2019.
[34] Alattabi, Z.R., Cahl, D., Voulgaris, G., "Swell and Wind Wave Inversion Using a Single Very High Frequency (VHF) Radar," *Journal of Atmospheric and Oceanic Technology*, Vol. 36, pp. 987-1013, 2019.
[35] Hasselmann, K., Barnett, TP., Bouws, E., Carlson, H., Cartwright, D.E., Enke, K., *et al.*, "Measurements of wind-wave growth and swell decay during the Joint North Sea Wave Project (JONSWAP)," Report Technique, pp. 1-95, 1973.